

This is the post-print version of the following article: Aires, A; Moller, M; Cortajarena, AL, [Protein Design for the Synthesis and Stabilization of Highly Fluorescent Quantum Dots](#), *Chem. Mater.* 2020, 32, 13, 5729–5738  
DOI: [10.1021/acs.chemmater.0c01484](https://doi.org/10.1021/acs.chemmater.0c01484)

This article may be used for non-commercial purposes in accordance with ACS Terms and Conditions for Self-Archiving.

# Protein design for the synthesis and stabilization of highly fluorescent quantum dots

Antonio Aires,<sup>\*,†</sup> Marco Moller,<sup>†</sup> and Aitziber L. Cortajarena<sup>\*,†,‡</sup>

<sup>†</sup> Center for Cooperative Research in Biomaterials (CIC biomaGUNE), Basque Research and Technology Alliance (BRTA), Paseo de Miramón 182, 20014, Donostia San Sebastián, Spain

<sup>‡</sup> Ikerbasque, Basque Foundation for Science, M<sup>a</sup> Díaz de Haro 3, 48013 Bilbao, Spain

**ABSTRACT:** Quantum dots (QDs) are studied intensively nowadays as fluorescent probes for biomedical applications due to their high emission quantum yield, excellent resistance to photo-bleaching, photo-stability and large Stokes shift, when contrasted with commonly utilized organic fluorescent dyes. This study introduces a protein engineering approach to incorporate metal coordination sites for the sustainable synthesis and stabilization of biocompatible CdS QDs in proteins. The resulting protein-stabilized CdS QDs (Prot-QDs), generated by a green aqueous route at 37 °C, are highly photo-luminescent and photo-stable, have a long shelf-life and high stability under physiological conditions. The Prot-QDs showed effective internalization and high fluorescence in cells, even at low doses, and biocompatibility. This work focuses on CdS QDs, since this composition has been extensively studied, however this approach could be easily translated to QDs with other metal composition. Here, protein design emerges as promising approach to generate protein-nanomaterial hybrids as broadly applicable tools in different applications such as light-emitting devices, metal ion detection, and biomedical applications.

## INTRODUCTION

Quantum dots (QDs) have received great attention because of their high emission quantum yields, excellent resistance to photo-bleaching, photo-stability, and large Stokes shifts, compared to traditional organic fluorescent dyes.<sup>1-5</sup> Lately, large efforts have been made to utilize QDs as fluorescent reporters for biomedical applications, for example, for bio-imaging.<sup>6-9</sup> However, conventional chemical QDs synthesis usually requires toxic reagents, organic solvents, extreme reaction conditions, intensive energy input, and relies on a series of cumbersome and time-consuming steps.<sup>10-11</sup> Additionally, after the chemical synthesis, QDs require post-synthetic processing to make them water soluble for biological applications.<sup>6,12</sup> Finally, most QDs synthesized by chemical methods present low biocompatibility and poor stability at high ionic strength conditions, thus significantly restricting their application.<sup>11,13-14</sup>

To overcome these limitations, continuous efforts have been made to develop eco-friendly and sustainable chemical strategies to synthesize QDs, that do not require harsh conditions or post-synthetic processing.<sup>15-17</sup> The currently described aqueous routes are critically-dependent on the use of surface capping agents. A wide range of organic molecules have been evaluated as capping agents, for example, organic thiols, including biological molecules, for example, cysteine, glutathione, amine-rich dendrimers, and polyphosphates.<sup>4</sup> Nevertheless, these methodologies produce QDs that still display low biocompatibility, sensitivity to pH and high ionic strength, as well as elevated production costs.<sup>18-20</sup> An alternative approach to template and stabilize QDs is to use peptides and proteins with high affinity for transition metals.<sup>21-23</sup> In nature, peptides rich in cysteines and glutamic acids, for example, phytochelatins participate

in the packaging and export of toxic cadmium as less harmful cadmium sulphide (CdS) nanocrystals.<sup>4</sup> Taking inspiration from biological strategies, peptide-assisted synthesis of QDs has become a promising method to grow semiconducting nanocrystals<sup>24-28</sup> and some examples have been reported on protein-QDs hybrids prepared by the direct synthesis of QDs in aqueous solution.<sup>4,23,25,29-32</sup> Proteins, such as BSA, lysozyme, trypsin, hemoglobin, transferrin, and poly-histidine fusion proteins have been used for the synthesis of protein-QDs hybrids.<sup>24,29,32-34</sup> However, the change of the established organic routes to more sustainable aqueous routes results in significantly decreased fluorescence quantum yields (QY).<sup>1,5,35-36</sup> Therefore, it is still challenging to produce biocompatible highly fluorescent QDs for biomedical applications.

Among the QDs, CdS is one of the most studied luminescent semiconductors due to their excellent optical and electrochemical properties, but the demonstrated toxicity of Cd has limited their biomedical applications. This study focuses on the engineering of protein scaffolds for the sustainable synthesis of biocompatible highly fluorescent CdS-QDs since even though many efforts have been made to develop sustainable strategies to synthesize CdS QDs,<sup>4,23,30-31</sup> the QY and biocompatibility required for their use in biomedical applications have not been achieved yet. In addition, the approach develop here for CdS, could be easily translated to QDs with more biocompatible metal composition.

The studies using proteins to stabilize QDs have demonstrated that different amino acids, including cysteine, glutamic acid, aspartic acid, and histidine bind Cd<sup>2+</sup> ions and nucleate CdS QDs.<sup>9-10,30-31</sup> However, to the best of our knowledge, the design of metal coordination sites into proteins for the synthe-

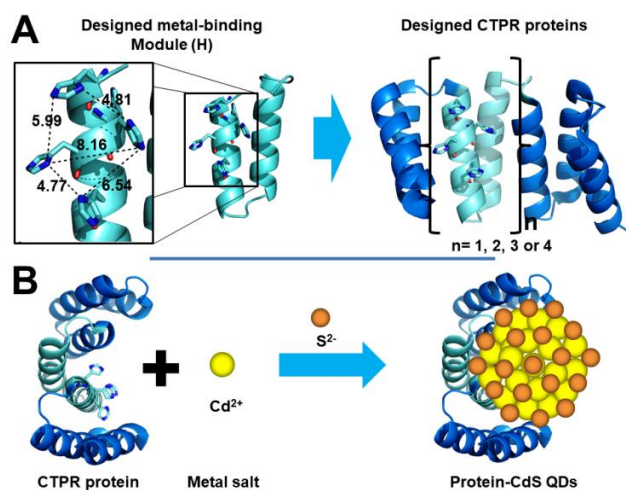


**Figure 1.** Design of CTPR proteins for the synthesis and stabilization of CdS QDs. **A.** Modified CTPR unit in which four histidines have been introduced at positions 2, 5, 6, and 9 (H module). Representation of the structure of the designed CTPR proteins constructed by combination of H (light blue) and W (blue) modules, based on the structure of CTPR3 (PDB ID: 1Na0). **B.** General scheme of the synthesis and stabilization of fluorescent CdS QDs by CTPR proteins.

sis of highly fluorescent biocompatible CdS QDs has never been approached. In this work, the design and incorporation of a metal coordination site into an engineered repeat protein is investigated for the sustainable synthesis and stabilization of CdS QDs with improved fluorescent properties, photo-stability, and biocompatibility that will enable their use in different applications such as light emitting devices,<sup>37-39</sup> metal ion detection,<sup>40-41</sup> and biomedical applications.<sup>3, 42-45</sup> A metal coordination site inspired in metalloproteins and based on four coordinating histidine residues was modeled on the crystal structure of a scaffold protein, the consensus tetratricopeptide repeat (CTPR) module.<sup>46</sup> Then arrays of repeat proteins containing different numbers of CTPR modules were assembled to explore the effect of the size of the metal coordination site. These designed repeat proteins were evaluated as novel stabilizing agents in the green synthesis of CdS QDs. Cysteines,<sup>31</sup> and glutamic acids<sup>30-31</sup> can also participate in cadmium coordination, thus CTPR modules with coordinating cysteines were constructed to evaluate the effect of the metal coordinating amino acid on the fluorescent properties of the protein-stabilized CdS QDs (Prot-QDs). The resulting Prot-QDs were fully characterized and their fluorescence properties, photo-stability and biocompatibility were tested *in vitro*. Overall, this work demonstrates the application of protein design strategies to generate biocompatible Prot-QDs with improved fluorescent properties and photo-stability as promising tools for broad-spectrum applications.

## RESULTS AND DISCUSSION

Based on previous works, which demonstrated that histidine can effectively bind  $\text{Cd}^{2+}$  ions to allow the formation and stabilization of QDs,<sup>32, 34, 54</sup> a metal coordination site composed by histidines was designed into an engineered repeat protein (CTPR). CTPR proteins present only a few highly conserved amino acids that encode the protein fold.<sup>55</sup> The amino acids at

the other positions permit variations, giving the flexibility to introduce novel functionalities such as different chemical reactivities and ligand-binding specificities.<sup>56</sup>

Bis-histidine, tris-histidine and tetra-histidine motifs are high-affinity motifs frequently observed in natural metalloproteins.<sup>57-63</sup> In addition, these motifs have been previously used for the nucleation and growth of nanomaterials into CTPR protein structure.<sup>64</sup> Therefore, a histidine-based designed metal binding site was modeled on the structure of the CTPR3 protein (1Na0).<sup>46</sup> The histidines were introduced at specific positions with modelled side chain conformations and backbone geometry of the metal-binding site compatible with the CTPR fold and with the desired metal coordination distances, observed in natural proteins' coordination sites ( $< 3\text{\AA}$ ),<sup>61, 65-66</sup> to bind  $\text{Cd}^{2+}$  ions (Figure 1A). In this case, four histidines were introduced at positions 2, 5, 6, and 9, generating the CTPR module H (Figure 1). The designed H module was integrated in CTPR proteins with one, two, three and four metal coordination units combining H modules and wild type CTPR modules (Wt), producing Wt(H)Wt, Wt(H)<sub>2</sub>Wt, Wt(H)<sub>3</sub>Wt and Wt(H)<sub>4</sub>Wt proteins (Figure 1). Finally, the potential of the designed proteins to bind enough  $\text{Cd}^{2+}$  ions for subsequent growing CdS QDs was validated computationally using the Metal Ion-Binding site prediction and docking server (<http://bioinfo.cmu.edu.tw/MIB/>).<sup>67</sup>

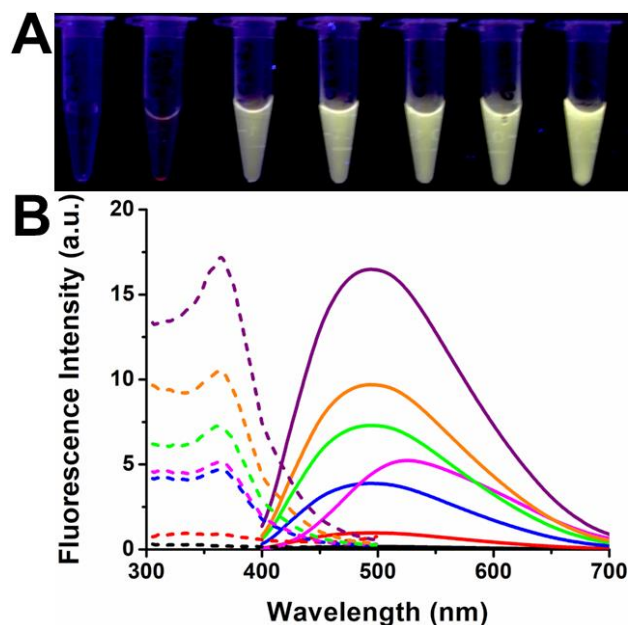


**Figure 2.** Fluorescence properties of the Prot-QDs synthesized with different CTPR proteins. (A) Photographs under UV-light ( $\lambda_{\text{ex}} = 365\text{ nm}$ ) of Prot-QDs. From left to right: Control without protein, (Wt)<sub>8</sub>, Wt(H)Wt, (Wt)<sub>8</sub>-histag, Wt(H)<sub>2</sub>Wt, Wt(H)<sub>3</sub>Wt, and Wt(H)<sub>4</sub>Wt. (B). Fluorescence excitation (dashed lines) and emission (solid lines) spectra of CdS QDs synthesized using (Wt)<sub>8</sub> (red), Wt(H)Wt (blue), (Wt)<sub>8</sub>-histag (magenta), Wt(H)<sub>2</sub>Wt (green), Wt(H)<sub>3</sub>Wt (orange) and Wt(H)<sub>4</sub>Wt (purple). A control experiment without protein is shown in black.

The capacity of the designed proteins to generate high fluorescence and photostable Prot-QDs was evaluated and compared with a control protein composed of eight identical Wt modules without metal coordination sites, (Wt)<sub>8</sub>, and with a

poly-histidine tagged control protein composed of eight identical Wt modules, (Wt)<sub>8</sub>-histag, since previous works showed the use of poly-his tags to stabilize fluorescent QDs.<sup>24, 33-34, 54</sup> Briefly, 2 mL of purified CTPR proteins (Figure S1) at 6.25  $\mu$ M were mixed with 100  $\mu$ L of Cd(CH<sub>3</sub>COO)<sub>2</sub> 100 mM at pH 10. After 60 min of incubation at room temperature, 400  $\mu$ L of Na<sub>2</sub>S 1.75mM were added dropwise (final protein: Cd: S molar ratio = 1:80:64), and the reaction was incubated in an orbital shaker incubator at 37 °C and 220 rpm for 5 days.

Finally, the Prot-QDs were purified via gel filtration using fast protein liquid chromatography (FPLC). The Prot-QDs formation was evaluated by the appearance of the characteristic fluorescence features of the QDs (Figure 2A). The fluorescence emission and excitation spectra of Prot-QDs are shown in Figure 2B.

The synthesis in absence of protein and, in presence of the control protein without metal coordination sites, (Wt)<sub>8</sub>, showed no fluorescence, whereas the synthesis in presence of a poly-histidine tagged control protein, (Wt)<sub>8</sub>-histag, and the designed CTPR proteins, showed emission peaks around 500-520 nm, when excited at 365 nm. An improvement of the fluorescent properties of the Prot-QDs was observed when the number of specific metal-binding sites (H modules) in the protein increased from 1 to 4 (Figure 2B), as well as when the number of total histidines increased from 4 to 16, when considering also the (Wt)<sub>8</sub>-histag. The synthesis using the protein with the largest number of coordinating histidines Wt(H)<sub>4</sub>Wt showed the largest photo-luminescence (PL). This template was selected for the optimization of synthetic parameters in a direct comparison with the poly-histidine fusion protein, (Wt)<sub>8</sub>-histag.

The influence of the metal:protein ratio (from 20:1 to 80:1) was assessed in the synthesis and stabilization of CdS QDs using the (Wt)<sub>8</sub>-histag and Wt(H)<sub>4</sub>Wt (Figure 3A). The largest fluorescence emission intensity of the Prot-QDs was observed at 80:1 ratio (Figure 3A). Metal:protein ratios larger than 80:1 caused protein aggregation and subsequent decrease in the fluorescence emission intensity. In addition, the influence of the Cd/Na<sub>2</sub>S ratio (from 1:0.4 to 1:1.6) on the fluorescent properties of the resulting Prot-QDs was evaluated using the Wt(H)<sub>4</sub>Wt protein (Figure S2). The largest fluorescence emission intensity of the Wt(H)<sub>4</sub>Wt-CdS was observed at 1:0.8 ratio (Figure S2A). Also, a red shift in the fluorescence emission of the Wt(H)<sub>4</sub>Wt-CdS was observed when the Cd/Na<sub>2</sub>S ratio was decreased from 1:0.4 to 1:1.6 (Figure S2B), which could be associated with an increase of nanocrystals size.<sup>23</sup> Under these optimized conditions, Wt(H)<sub>4</sub>Wt protein mediated the formation of CdS QDs with a QY of 32%, 2.8-fold brighter than those obtained with (Wt)<sub>8</sub>-histag (QY= 11%) (Figure 2B). This QY is remarkably high compared to those of previously reported CdS QDs synthesized by aqueous routes (QY= 2.0-7.5%).<sup>23, 68-70</sup> To better understand the excited-state dynamics of the Prot-QDs, time-resolved PL measurements were performed. Tri-exponential fit of the PL decay curves (Figure S3), provided 104 $\pm$ 2 and 127 $\pm$ 3 ns amplitude-weighted average lifetimes for (Wt)<sub>8</sub>-histag-CdS QDs and

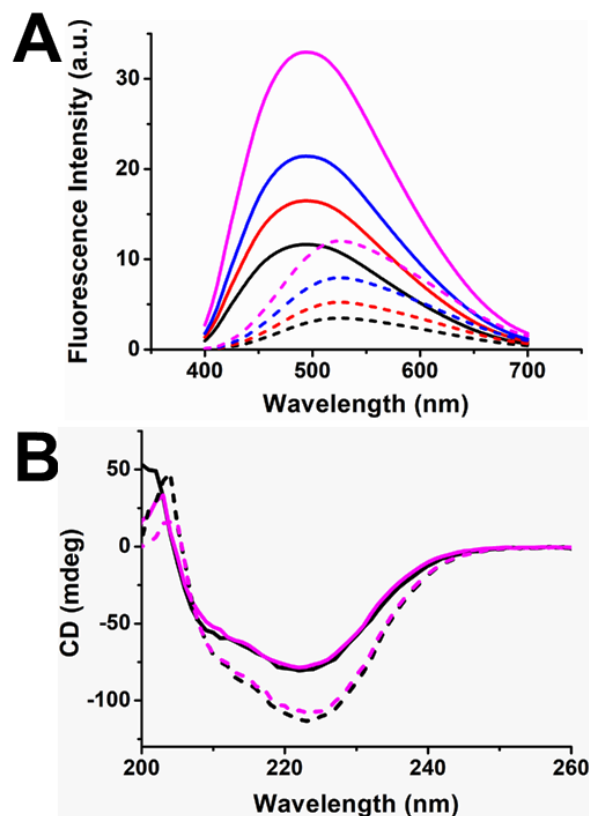


**Figure 3.** A. Fluorescence spectra of the Prot-QDs synthesized with the Wt(H)<sub>4</sub>Wt protein (solid lines) and (Wt)<sub>8</sub>-histag protein (dash lines) using metal:protein ratios of 20:1 (black), 40:1 (red), 60:1 (blue), and 80:1 (magenta). All spectra were acquired using an  $\lambda_{exc}$ : 365nm. B. CD spectra of Wt(H)<sub>4</sub>Wt (black solid line) (Wt)<sub>8</sub>-histag (black dash line) proteins and Wt(H)<sub>4</sub>Wt-CdS (magenta solid line) and (Wt)<sub>8</sub>-histag-CdS (magenta dash line) QDs synthesized using a metal:protein ratio of 80:1. All spectra were recorded at 20  $\mu$ M protein concentration and at 25 °C.

Wt(H)<sub>4</sub>Wt-CdS QDs, respectively (Figure S3 and Table S1), in agreement with the complex multi-component and relatively long lifetimes previously reported for QDs.<sup>5, 71-73</sup> These long lifetimes make the CTPR-based Prot-QDs interesting candidates for biomedical applications.<sup>74</sup>

The structural integrity of the CTPR protein template upon CdS QDs synthesis, was confirmed by circular dichroism (CD). CD spectra of Wt(H)<sub>4</sub>Wt-CdS QDs and (Wt)<sub>8</sub>-histag-CdS QDs showed the signature of  $\alpha$ -helical structure (Figure 3B). Therefore, additional functional properties, critical for future applications, could be encoded into the protein template together with the QD stabilization domains.<sup>75-77</sup>

In order to study the effect of the metal coordinating residue of the protein in the fluorescent properties of the Prot-QDs, and to explore the tunability of the QDs properties by the protein template, four cysteines were introduced in the coordination site, generating the module C. The resulting Wt(C)<sub>4</sub>Wt protein was evaluated in the synthesis and stabilization of CdS QDs. Figure S2 shows that the fluorescence emission of the CdS QDs stabilized by cysteines is lower than the Prot-QDs stabilized by Wt(H)<sub>4</sub>Wt. Accordingly, the QY of the Prot-QDs was reduced (QY=24%) when cysteines are the metal coordinating residues (Figure S4), compared to the previously described (QY=32%)



for histidine coordination. The PL lifetime (LT) is slightly lower, LT=127±3 ns for C6-16His and LT=114±2 ns for Wt(C)<sub>4</sub>Wt (Figure S3). These results show the relevance of the nature of coordinating residues in the final properties of the fluorescent Prot-QDs, and the great potential of protein design when applied to the generation of templates for tunable and controlled synthesis of QDs. In accordance with these data, previously reported studies on the synthesis and stabilization of semiconductor nanocrystals have shown that thiol-based ligands tend to negatively affect the PL properties of the hydrophilic QDs.<sup>78-80</sup> Moreover, under ambient conditions, most thiol-based ligands can be affected by photo-oxidation during extended storage time, which causes ligand desorption from the QD surface.<sup>81-85</sup> On the other hand, the capping of semiconductor QDs with thiols is known to quench PL through a process attributed to the introduction of hole traps.<sup>86-87</sup>

The chemical composition of the Prot-QDs (table S2) was determined by inductively coupled plasma mass spectrometry (ICP-MS) for the Cd content (Table S3) and elemental analysis for the S content (Table S4). Table S2 shows the chemical composition of (Wt)<sub>8</sub>-histag-CdS, Wt(H)<sub>4</sub>Wt-CdS, and Wt(C)<sub>4</sub>Wt-CdS. For all the protein templates the resulting QDs presented between 61-82 atoms per QD with a S:Cd stoichio-

metry around 1:1.5, which can be described as Cd-rich QDs.<sup>79, 88</sup> This feature may determine their excellent PL properties, since previous works demonstrated that Cd-rich CdS QDs present better PL properties than the S-rich CdS QDs.<sup>66, 75</sup> The size and the morphology of the Prot-QDs were evaluated by transmission electron microscopy (TEM). TEM images confirmed that the Prot-QDs were spherical particles with excellent monodispersity (Figure 4A-C). Size distribution analysis revealed that the diameters of (Wt)<sub>8</sub>-histag-CdS, Wt(H)<sub>4</sub>Wt-CdS and Wt(C)<sub>4</sub>Wt-CdS QDs were 2.0±0.5, 1.9±0.4, and 2.1±0.6 nm, respectively (Figure 4D-F). Further, size and morphology of the Prot-QDs were confirmed by scanning transmission electron microscopy (STEM), taking advantage of the chemical contrast of Cd and S in high-angle annular dark field (HAADF) (Figure S5). Energy dispersive X-ray spectroscopy (EDX) enabled the detection of the different elements on the surface of the QDs. The EDX spectra of the Prot-QDs verified the presence of Cd and S in all the samples (Figure S6).

The photo-stability, storage stability, stability under physiological conditions and bio-compatibility of fluorescent probes are critically important for different applications. To explore the applicability of these Prot-QDs in bio-imaging and biolabeling, first the photo-stability of the Prot-QDs was tested in comparison with glutathione reduced capped CdS QDs (GSH-CdS),<sup>23, 89-90</sup> synthesized through the same experimental procedure as a control of non-protein stabilized CdS QDs (Supplementary information, Figures S7-8), and with a dye commonly used in cell labeling (DAPI). GSH-CdS presented an emission peak at 570 nm, when excited at 380 nm, a diameter of 2.0±0.5nm, and a QY of 8%, 4-fold less bright than those obtained with the Wt(H)<sub>4</sub>Wt protein. The Prot-QDs, GSH-CdS and DAPI were continuously excited at 365 nm with a Xenon flash lamp (20 kW) and the PL spectra were recorded at different time points. After 60 min of light exposure, the PL intensities of the (Wt)<sub>8</sub>-histag-CdS, Wt(H)<sub>4</sub>Wt-CdS, Wt(C)<sub>4</sub>Wt-CdS, GSH-CdS QDs and DAPI decreased to 75, 82, 72, 32 and 70 % of the initial signal, respectively (Figure S9). In addition, the Prot-QDs presented excellent stability under storage conditions, with no significant change in their fluorescent emission intensity after 30 days at 4 °C in PBS (Figure S10). Then, the stability of the Prot-QDs under physiological simulated conditions at 37 °C was evaluated in comparison with GSH-CdS. Under physiological simulated conditions the PL of (Wt)<sub>8</sub>-histag-CdS QDs and Wt(C)<sub>4</sub>Wt-CdS QDs decreased to 34% and 50% in PBS, and to 50% and 65% in serum-containing medium (SCM) (Figure S11). Notably, the PL of Wt(H)<sub>4</sub>Wt-CdS QDs was retained above 80% after 7 days in both media. Finally, GSH-CdS QDs presented poor stability in both media and their PL decreased to 8% in PBS and to 15% in SCM after 7 days on incubation (Figure S11). These results show the relevance of the position and nature of the coordinating residues in the protein template to the stability under physiological simulated conditions and to the photo-stability of the Prot-QDs. Furthermore, the feasibility of Wt(H)<sub>4</sub>Wt-CdS QDs for live *in vitro* imaging was evaluated on account of their notable fluorescence and bio-compatible protein coating. *In vitro* biocompatibility and the cellular uptake of Wt(H)<sub>4</sub>Wt-CdS QDs were evaluated in MDA-MB-231 breast cancer cells at different concentrations ([protein]: 0.5-20 μM; [Cd]: 25-1000 μM), in comparison with (Wt)<sub>8</sub>-histag-CdS, Wt(C)<sub>4</sub>Wt-CdS and GSH-CdS QDs ([Cd]: 25-

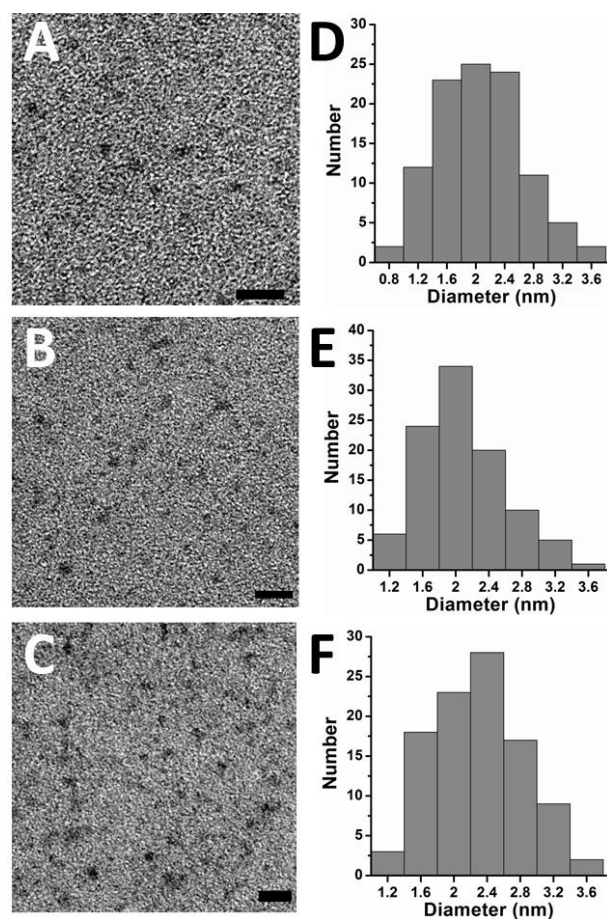


**Figure 4.** TEM images and size distribution histograms (determined by measuring 100 particles in the TEM images, n=3) of (Wt)<sub>8</sub>-histag-CdS QDs (A, D), Wt(H)<sub>4</sub>Wt-CdS QDs (B, E), and Wt(C)<sub>4</sub>Wt-CdS QDs (C, F). Scale Bars 10 nm.

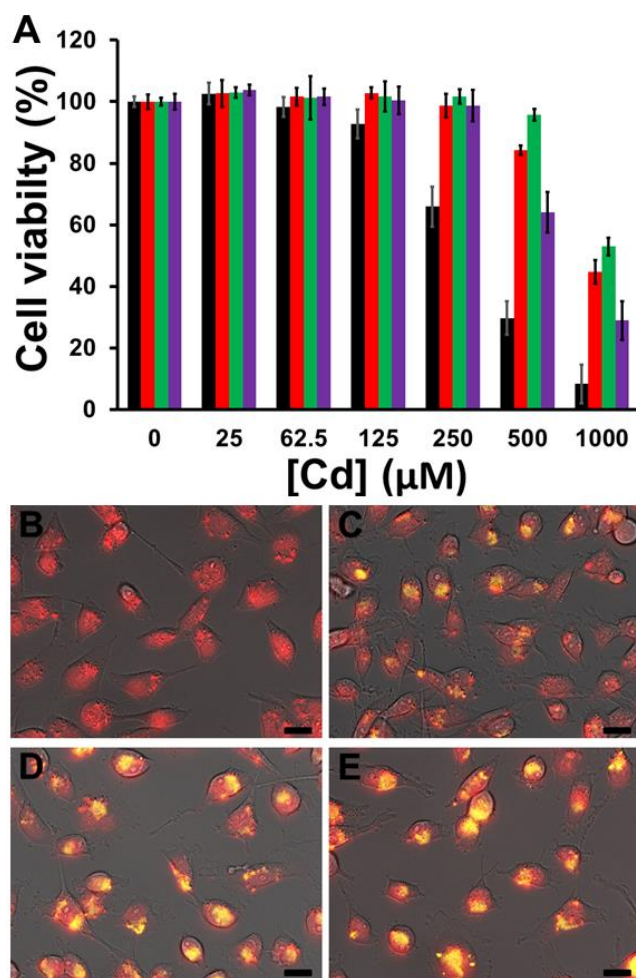


**Figure 5.** A. Cytotoxicity of CdS QDs on MDA-MB-231 breast cancer cells measured by Alamar blue assay after 5 days of incubation. (Wt)<sub>8</sub>-Histag-CdS (Black), Wt(H)<sub>4</sub>Wt-CdS (red), Wt(C)<sub>4</sub>Wt-CdS (green) and GSH-CdS QDs (purple) (n=3). B-E. Live fluorescence microscopy images of MDA-MB-231 breast cancer cells incubated with metal Wt(H)<sub>4</sub>Wt-CdS. Control cells (B) and cells incubated with Wt(H)<sub>4</sub>Wt-CdS at 0.5 μM (C), 1 μM (D), and 2.5 μM (E) for 4 h. The Wt(H)<sub>4</sub>Wt-CdS fluorescence is shown in yellow emission under excitation at 370 nm. In red is shown the nuclear staining with NucRed™ Live 647 upon excitation with a red laser (633 nm). Scale bars correspond to 20 μM.

1000 μM), under standard cell culture conditions. Prot-QDs and GSH-CdS presented an efficient internalization in breast cancer cells after 24 hours of incubation (Figure S12). These results represented a total internalization of  $28 \pm 19$ ,  $22 \pm 16$ ,  $17 \pm 11$  and  $15 \pm 8$  % for (Wt)<sub>8</sub>-histag-CdS, Wt(H)<sub>4</sub>Wt-CdS, Wt(C)<sub>4</sub>Wt-CdS and GSH-CdS QDs, respectively (average cell internalization at six different CdS concentrations). Then, after 5 days of incubation, cells exposed to Wt(H)<sub>4</sub>Wt-CdS QDs did not induce cytotoxicity nor promoted morphological changes in cells at concentrations lower than 500 μM of Cd ([Protein]: 10 μM), and showed at 1000 μM of Cd ([Protein]: 20 μM) a reduction of  $55 \pm 4$  % in the cell viability (Figure 5A). Figure 5A shows that Wt(H)<sub>4</sub>Wt-CdS presented better biocompatibility than the CdS stabilized by Wt(C)<sub>4</sub>Wt and poly-histidine tagged control proteins, and GHS, taking into account the level of CdS internalization (Figure S12). The concentration of Cd required to kill 50% of the tested cells (IC<sub>50</sub> values), extrapolated from Figure S13, were 360 μM for (Wt)<sub>8</sub>-histag-CdS, 940 μM for

Wt(H)<sub>4</sub>Wt-CdS, 1030 μM for Wt(C)<sub>4</sub>Wt-CdS, and 700 μM for GSH-CdS QDs, respectively. These IC<sub>50</sub> values corresponded to a total internalization of  $33 \pm 2$  of Cd per cell for (Wt)<sub>8</sub>-histag-CdS,  $36 \pm 2$  fg of Cd per cell for Wt(H)<sub>4</sub>Wt-CdS,  $26 \pm 1$  fg of Cd per cell for Wt(C)<sub>4</sub>Wt-CdS, and  $25 \pm 2$  fg of Cd per cell for GSH-CdS QDs, respectively (extrapolated from Figure S12). Finally, the bio-imaging experiments were performed at Prot-QDs concentrations below cytotoxic levels (0.5-2.5 μM of Wt(H)<sub>4</sub>Wt-CdS QDs). After 4 hours incubation with the Prot-QDs the cells were stained with a nuclear marker for 30 min and imaged by live fluorescence microscopy after thorough washing with PBS to remove uninternalized Prot-QDs (Figure 5B-E). All the cells treated with Prot-QDs showed yellow fluorescence even at the lowest concentration tested (Figures 5C-E), compared to non-treated cells (Figure 5B). These results endorse the biocompatible nature of Wt(H)<sub>4</sub>Wt-CdS QDs at doses lower than 10 μM and clearly demonstrate their efficacy to label live cells at those biocompatible concentrations.

## CONCLUSIONS

During the last decade, the scientific and industrial interest to develop more sustainable methods to synthesize QDs has grown. Nevertheless, these new expensive methods produce QDs that still display low biocompatibility and low stability under physiological conditions. Several chemical procedures based on biological reagents and mild reaction conditions have been developed during the last years.<sup>15-20</sup> In addition, these procedures have contributed to improve the biocompatibility of QDs. However, the quality, in terms of PL intensity, of the fluorescent QDs synthesized by these simpler and eco-friendly methods decreases in comparison with those obtained by traditional organic chemical route.<sup>1, 5, 35-36</sup>

This work validates protein engineering as a new approach for the sustainable synthesis and stabilization of high-quality fluorescent QDs by an eco-friendly and sustainable aqueous route. This study focuses on CdS QDs, since this composition has been extensively studied, however this approach could be easily translated to QDs with other metal composition. Here, a versatile approach to design proteins for the green synthesis of highly fluorescent CdS QDs has been developed by the incorporation of specific metal coordination sites that rely on histidines and cysteines. This approach shows that the design of engineered protein templates not only improves the PL properties of Prot-QDs, but also improves their photo-stability, stability under physiological simulated conditions, and biocompatibility, in comparison with a poly-histidine fusion protein and GSH. The resulting engineered Prot-QDs, generated by a green aqueous route at 37 °C, are highly photo-luminescent and photo-stable, have a long shelf life, are stable under physiological simulated conditions and display high biocompatibility, as well as low production costs. Finally, the Prot-QDs are able to enter into living cells, showing great cell labeling capacity at very low doses without affecting cell viability, making them useful tools for biomedical applications. In addition, the approach developed in this work could be translated into other protein cage architectures (presenting α-helices structures),<sup>47</sup> that have been previously used as templates for the synthesis of different nanomaterials,<sup>47-53</sup> to tune the properties of the resulted protein-hybrid nanomaterial for their application in different fields.



## ASSOCIATED CONTENT

### Supporting Information

The Supporting Information is available free of charge on the ACS Publications website at DOI: [10.1021/acs.chemmater.0c01484](https://doi.org/10.1021/acs.chemmater.0c01484).  
Synthetic procedures and characterization data of all CdS QDs.

## AUTHOR INFORMATION

### Corresponding Author

\* [alcortajarena@cicbiomagune.es](mailto:alcortajarena@cicbiomagune.es); [aares@cicbiomagune.es](mailto:aares@cicbiomagune.es).

### Notes

The authors declare no competing financial interest.

## ACKNOWLEDGMENT

This work was partially supported by the European Research Council ERC-CoG-648071-ProNANO, ERC-PoC-841063-NIMM, the Spanish Ministry of Economy and Competitiveness (BIO2016-77367-R) (ALC), and the Basque Government (Elkartek KK-2017/00008). This work was performed under the Maria de Maeztu Units of Excellence Program from the Spanish State Research Agency – Grant No. MDM-2017-0720 (CIC biomaGUNE). We thank Dr. I. Llaena, Dr. J. Calvo, and Dr. D. Otaegui at CIC biomaGUNE for support with the acquisition of fluorescence microscopy images and mass spectrometry measurements.

## REFERENCES

1. Chan, W. C., Quantum Dot Bioconjugates for Ultrasensitive Nonisotopic Detection. *Science* **1998**, *281* (5385), 2016-2018.
2. Gao, X.; Cui, Y.; Levenson, R. M.; Chung, L. W. K.; Nie, S., In vivo cancer targeting and imaging with semiconductor quantum dots. *Nature Biotechnology* **2004**, *22* (8), 969-976.
3. Michalet, X., Quantum Dots for Live Cells, in Vivo Imaging, and Diagnostics. *Science* **2005**, *307* (5709), 538-544.
4. Spoerke, E. D.; Voigt, J. A., Influence of Engineered Peptides Cadmium Sulfide Nanocrystals. *Advanced Functional Materials* **2007**, *17* (13), 2031-2037.
5. Resch-Genger, U.; Grabolle, M.; Cavaliere-Jaricot, S.; Nitschke, R.; Nann, T., Quantum dots versus organic dyes as fluorescent labels. *Nature Methods* **2008**, *5* (9), 763-775.
6. Medintz, I. L.; Uyeda, H. T.; Goldman, E. R.; Mattoussi, H., Quantum dot bioconjugates for imaging, labelling and sensing. *Nature Materials* **2005**, *4* (6), 435-446.
7. So, M.-K.; Xu, C.; Loening, A. M.; Gambhir, S. S.; Rao, J., Self-illuminating quantum dot conjugates for in vivo imaging. *Nature Biotechnology* **2006**, *24* (3), 339-343.
8. Martynenko, I. V.; Litvin, A. P.; Purcell-Milton, F.; Baranov, A. V.; Fedorov, A. V.; Gun'ko, Y. K., Application of semiconductor quantum dots in bioimaging and biosensing. *Journal of Materials Chemistry B* **2017**, *5* (33), 6701-6727.
9. Kairdolf, B. A.; Smith, A. M.; Stokes, T. H.; Wang, M. D.; Young, A. N.; Nie, S., Semiconductor Quantum Dots for Bioimaging and Biodiagnostic Applications. *Annual Review of Analytical Chemistry* **2013**, *6* (1), 143-162.
10. Biju, V.; Itoh, T.; Anas, A.; Sujith, A.; Ishikawa, M., Semiconductor quantum dots and metal nanoparticles: syntheses, optical properties, and biological applications. *Analytical and Bioanalytical Chemistry* **2008**, *391* (7), 2469-2495.
11. Peng, Z. A.; Peng, X., Formation of High-Quality CdTe, CdSe, and CdS Nanocrystals Using CdO as Precursor. *Journal of the American Chemical Society* **2001**, *123* (1), 183-184.
12. Liu, W.; Howarth, M.; Greytak, A. B.; Zheng, Y.; Nocera, D. G.; Ting, A. Y.; Bawendi, M. G., Compact Biocompatible Quantum Dots Functionalized for Cellular Imaging. *Journal of the American Chemical Society* **2008**, *130* (4), 1274-1284.
13. Mo, D.; Hu, L.; Zeng, G.; Chen, G.; Wan, J.; Yu, Z.; Huang, Z.; He, K.; Zhang, C.; Cheng, M., Cadmium-containing quantum dots:

properties, applications, and toxicity. *Applied Microbiology and Biotechnology* **2017**, *101* (7), 2713-2733.

14. Wang, J.; Long, Y.; Zhang, Y.; Zhong, X.; Zhu, L., Preparation of Highly Luminescent CdTe/CdS Core/Shell Quantum Dots. *ChemPhysChem* **2009**, *10* (4), 680-685.
15. Zheng, Y.; Yang, Z.; Ying, J. Y., Aqueous Synthesis of Glutathione-Capped ZnSe and Zn<sub>1-x</sub>Cd<sub>x</sub>Se Alloyed Quantum Dots. *Advanced Materials* **2007**, *19* (11), 1475-1479.
16. Sheng, Z.; Chen, L., Switch-on fluorescent strategy based on crystal violet-functionalized CdTe quantum dots for detecting L-cysteine and glutathione in water and urine. *Analytical and Bioanalytical Chemistry* **2017**, *409* (26), 6081-6090.
17. Aboulaich, A.; Balan, L.; Ghanbaja, J.; Medjahdi, G.; Merlin, C.; Schneider, R. I., Aqueous Route to Biocompatible ZnSe:Mn/ZnO Core/Shell Quantum Dots Using 1-Thioglycerol As Stabilizer. *Chemistry of Materials* **2011**, *23* (16), 3706-3713.
18. Singh, G.; Kumar, M.; Soni, U.; Arora, V.; Bansal, V.; Gupta, D.; Bhat, M.; Dinda, A. K.; Sapra, S.; Singh, H., Cancer Cell Targeting Using Folic Acid/Anti-HER2 Antibody Conjugated Fluorescent CdSe/CdS/ZnS-Mercaptopropionic Acid and CdTe-Mercaptosuccinic Acid Quantum Dots. *Journal of Nanoscience and Nanotechnology* **2016**, *16* (1), 130-143.
19. Díaz, V.; Ramírez-Maureira, M.; Monrás, J. P.; Vargas, J.; Bravo, D.; Osorio-Román, I. O.; Vásquez, C. C.; Pérez-Donoso, J. M., Spectroscopic Properties and Biocompatibility Studies of CdTe Quantum Dots Capped with Biological Thiols. *Science of Advanced Materials* **2012**, *4* (5), 609-616.
20. Hardman, R., A Toxicologic Review of Quantum Dots: Toxicity Depends on Physicochemical and Environmental Factors. *Environmental Health Perspectives* **2006**, *114* (2), 165-172.
21. Whaley, S. R.; English, D. S.; Hu, E. L.; Barbara, P. F.; Belcher, A. M., Selection of peptides with semiconductor binding specificity for directed nanocrystal assembly. *Nature* **2000**, *405* (6787), 665-668.
22. Flynn, C. E.; Mao, C.; Hayhurst, A.; Williams, J. L.; Georgiou, G.; Iverson, B.; Belcher, A. M., Synthesis and organization of nanoscale II-VI semiconductor materials using evolved peptide specificity and viral capsid assembly. *J. Mater. Chem.* **2003**, *13* (10), 2414-2421.
23. Dunleavy, R.; Lu, L.; Kiely, C. J.; McIntosh, S.; Berger, B. W., Single-enzyme biomineralization of cadmium sulfide nanocrystals with controlled optical properties. *Proceedings of the National Academy of Sciences* **2016**, *113* (19), 5275-5280.
24. Zhou, W.; Baneyx, F., Biofabrication of ZnS:Mn luminescent nanocrystals using histidine, hexahistidine, and His-tagged proteins: A comparison study. *Biochemical Engineering Journal* **2014**, *89*, 28-32.
25. Dameron, C. T.; Winge, D. R., Characterization of peptide-coated cadmium-sulfide crystallites. *Inorganic Chemistry* **1990**, *29* (7), 1343-1348.
26. Kramer, R. M.; Li, C.; Carter, D. C.; Stone, M. O.; Naik, R. R., Engineered Protein Cages for Nanomaterial Synthesis. *Journal of the American Chemical Society* **2004**, *126* (41), 13282-13286.
27. Naik, R. R.; Jones, S. E.; Murray, C. J.; McAuliffe, J. C.; Vaia, R. A.; Stone, M. O., Peptide Templates for Nanoparticle Synthesis Derived from Polymerase Chain Reaction-Driven Phage Display. *Advanced Functional Materials* **2004**, *14* (1), 25-30.
28. Katz, E.; Willner, I., Integrated Nanoparticle-Biomolecule Hybrid Systems: Synthesis, Properties, and Applications. *Angewandte Chemie International Edition* **2004**, *43* (45), 6042-6108.
29. Lee, J. Y.; Kim, J. S.; Park, J. C.; Nam, Y. S., Protein-quantum dot nanohybrids for bioanalytical applications. *Wiley Interdisciplinary Reviews: Nanomedicine and Nanobiotechnology* **2016**, *8* (2), 178-190.
30. Naito, M.; Iwahori, K.; Miura, A.; Yamane, M.; Yamashita, I., Circularly Polarized Luminescent CdS Quantum Dots Prepared in a Protein Nanocage. *Angewandte Chemie International Edition* **2010**, *49* (39), 7006-7009.
31. Spreitzer, G.; Whitting, J. M.; Madura, J. D.; Wright, D. W., Peptide-encapsulated CdS nanoclusters from a combinatorial ligand library. *Chemical Communications* **2000**, (3), 209-210.
32. Wei, H.; House, S.; Wu, J.; Zhang, J.; Wang, Z.; He, Y.; Gao, E. J.; Gao, Y.; Robinson, H.; Li, W.; Zuo, J.; Robertson, I. M.; Lu, Y., Enhanced and tunable fluorescent quantum dots within a single crystal of protein. *Nano Research* **2013**, *6* (9), 627-634.

33. He, X.; Gao, L.; Ma, N., One-Step Instant Synthesis of Protein-Conjugated Quantum Dots at Room Temperature. *Scientific Reports* **2013**, *3* (1).
34. Aryal, B. P.; Benson, D. E., Polyhistidine fusion proteins can nucleate the growth of CdSe nanoparticles. *Bioconjugate chemistry* **2007**, *18* (2), 585-9.
35. Xuan, T.; Wang, X.; Liu, J.; Li, H.; Pan, L.; Sun, Z., One-pot synthesis of high quality CdS nanocrystals by microwave irradiation in an organic phase: a green route for mass production. *Journal of Materials Chemistry C* **2013**, *1* (30), 4550.
36. Jing, L.; Kershaw, S. V.; Li, Y.; Huang, X.; Li, Y.; Rogach, A. L.; Gao, M., Aqueous Based Semiconductor Nanocrystals. *Chemical Reviews* **2016**, *116* (18), 10623-10730.
37. Ilaiyaraja, P.; Mocherla, P. S. V.; Srinivasan, T. K.; Sudakar, C., Synthesis of Cu-Deficient and Zn-Graded Cu-In-Zn-S Quantum Dots and Hybrid Inorganic-Organic Nanophosphor Composite for White Light Emission. *ACS Applied Materials & Interfaces* **2016**, *8* (19), 12456-12465.
38. Bhandari, S.; Pramanik, S.; Khandelia, R.; Chattopadhyay, A., Gold Nanocluster and Quantum Dot Complex in Protein for Biofriendly White-Light-Emitting Material. *ACS Applied Materials & Interfaces* **2016**, *8* (3), 1600-1605.
39. Huo, S.; Duan, P.; Jiao, T.; Peng, Q.; Liu, M., Self-Assembled Luminescent Quantum Dots To Generate Full-Color and White Circularly Polarized Light. *Angewandte Chemie International Edition* **2017**, *56* (40), 12174-12178.
40. Prasuhn, D. E.; Feltz, A.; Blanco-Canosa, J. B.; Susumu, K.; Stewart, M. H.; Mei, B. C.; Yakovlev, A. V.; Loukou, C.; Mallet, J.-M.; Oheim, M.; Dawson, P. E.; Medintz, I. L., Quantum Dot Peptide Biosensors for Monitoring Caspase 3 Proteolysis and Calcium Ions. *ACS Nano* **2010**, *4* (9), 5487-5497.
41. Jurado-Sánchez, B.; Escarpa, A.; Wang, J., Lighting up micromotors with quantum dots for smart chemical sensing. *Chemical Communications* **2015**, *51* (74), 14088-14091.
42. Bruchez Jr, M., Semiconductor Nanocrystals as Fluorescent Biological Labels. *Science* **1998**, *281* (5385), 1013-1016.
43. Michalska, M.; Florczak, A.; Dams-Kozłowska, H.; Gapinski, J.; Jurga, S.; Schneider, R., Peptide-functionalized ZCIS QDs as fluorescent nanoprobe for targeted HER2-positive breast cancer cells imaging. *Acta Biomaterialia* **2016**, *35*, 293-304.
44. Manshian, B. B.; Jiménez, J.; Himmelreich, U.; Soenen, S. J., Personalized medicine and follow-up of therapeutic delivery through exploitation of quantum dot toxicity. *Biomaterials* **2017**, *127*, 1-12.
45. Chinnathambi, S.; Shirahata, N., Recent advances on fluorescent biomarkers of near-infrared quantum dots for in vitro and in vivo imaging. *Science and Technology of Advanced Materials* **2019**, *20* (1), 337-355.
46. Main, E. R. G.; Xiong, Y.; Cocco, M. J.; D'Andrea, L.; Regan, L., Design of Stable  $\alpha$ -Helical Arrays from an Idealized TPR Motif. *Structure* **2003**, *11* (5), 497-508.
47. Qazi, S.; Lucon, J.; Uchida, M.; Douglas, T., Protein Cage Nanoparticles for Hybrid Inorganic-Organic Materials. **2013**, 273-304.
48. Douglas, T.; Dickson, D. P. E.; Betteridge, S.; Charnock, J.; Garner, C. D.; Mann, S., Synthesis and Structure of an Iron(III) Sulfide-Ferritin Bioinorganic Nanocomposite. *Science* **1995**, *269* (5220), 54-57.
49. Meldrum, F.; Heywood, B.; Mann, S., Magnetoferritin: in vitro synthesis of a novel magnetic protein. *Science* **1992**, *257* (5069), 522-523.
50. Shenton, W.; Mann, S.; Cölfen, H.; Bacher, A.; Fischer, M., Synthesis of Nanophase Iron Oxide in Lumazine Synthase Capsids. *Angewandte Chemie International Edition* **2001**, *40* (2), 442-445.
51. Wong, K. K. W.; Mann, S., Biomimetic synthesis of cadmium sulfide-ferritin nanocomposites. *Advanced Materials* **1996**, *8* (11), 928-932.
52. Allen, M.; Willits, D.; Young, M.; Douglas, T., Constrained Synthesis of Cobalt Oxide Nanomaterials in the 12-Subunit Protein Cage from *Listeria innocua*. *Inorganic Chemistry* **2003**, *42* (20), 6300-6305.
53. Kang, S.; Lucon, J.; Varpness, Z. B.; Liepold, L.; Uchida, M.; Willits, D.; Young, M.; Douglas, T., Monitoring Biomimetic Platinum Nanocluster Formation Using Mass Spectrometry and Cluster-Dependent H<sub>2</sub> Production. *Angewandte Chemie International Edition* **2008**, *47* (41), 7845-7848.
54. Jia, J.; Zhang, P.; Gao, D.; Sheng, Z.; Hu, D.; Gong, P.; Wu, C.; Chen, J.; Cai, L., One-step synthesis of peptide-programmed QDs as ready-to-use nanoprobe. *Chemical Communications* **2013**, *49* (40), 4492.
55. Magliery, T. J.; Regan, L., Beyond Consensus: Statistical Free Energies Reveal Hidden Interactions in the Design of a TPR Motif. *Journal of Molecular Biology* **2004**, *343* (3), 731-745.
56. Cortajarena, A. L.; Liu, T. Y.; Hochstrasser, M.; Regan, L., Designed Proteins To Modulate Cellular Networks. *ACS Chemical Biology* **2010**, *5* (6), 545-552.
57. Arnold, F.; Haymore, B., Engineered metal-binding proteins: purification to protein folding. *Science* **1991**, *252* (5014), 1796-1797.
58. Lu, Y.; Yeung, N.; Sieracki, N.; Marshall, N. M., Design of functional metalloproteins. *Nature* **2009**, *460* (7257), 855-862.
59. Strange, R. W.; Blackburn, N. J.; Knowles, P. F.; Hasnain, S. S., X-ray absorption spectroscopy of metal-histidine coordination in metalloproteins. Exact simulation of the EXAFS of tetrakis(imidazole)copper(II) nitrate and other copper-imidazole complexes by the use of a multiple-scattering treatment. *Journal of the American Chemical Society* **1987**, *109* (23), 7157-7162.
60. Lu, Y.; Berry, S. M.; Pfister, T. D., Engineering Novel Metalloproteins: Design of Metal-Binding Sites into Native Protein Scaffolds. *Chemical Reviews* **2001**, *101* (10), 3047-3080.
61. Dokmanić, I.; Šikić, M.; Tomić, S., Metals in proteins: correlation between the metal-ion type, coordination number and the amino-acid residues involved in the coordination. *Acta Crystallographica Section D Biological Crystallography* **2008**, *64* (3), 257-263.
62. Regan, L., The Design of Metal-Binding Sites in Proteins. *Annual Review of Biophysics and Biomolecular Structure* **1993**, *22* (1), 257-281.
63. Regan, L., Protein design: novel metal-binding sites. *Trends in Biochemical Sciences* **1995**, *20* (7), 280-285.
64. Aires, A.; Llaena, I.; Moller, M.; Castro-Smirnov, J.; Cabanillas-Gonzalez, J.; Cortajarena, A. L., A Simple Approach to Design Proteins for the Sustainable Synthesis of Metal Nanoclusters. *Angewandte Chemie International Edition* **2019**, *58* (19), 6214-6219.
65. Andreini, C.; Cavallaro, G.; Lorenzini, S.; Rosato, A., MetalPDB: a database of metal sites in biological macromolecular structures. *Nucleic Acids Research* **2012**, *41* (D1), D312-D319.
66. Zheng, H.; Chruszcz, M.; Lasota, P.; Lebiada, L.; Minor, W., Data mining of metal ion environments present in protein structures. *Journal of Inorganic Biochemistry* **2008**, *102* (9), 1765-1776.
67. Lin, Y.-F.; Cheng, C.-W.; Shih, C.-S.; Hwang, J.-K.; Yu, C.-S.; Lu, C.-H., MIB: Metal Ion-Binding Site Prediction and Docking Server. *Journal of Chemical Information and Modeling* **2016**, *56* (12), 2287-2291.
68. Yang, Z.; Lu, L.; Berard, V. F.; He, Q.; Kiely, C. J.; Berger, B. W.; McIntosh, S., Biomanufacturing of CdS quantum dots. *Green Chemistry* **2015**, *17* (7), 3775-3782.
69. Li, H.; Shih, W. H.; Shih, W. Y.; Chen, L.; Tseng, S. J.; Tang, S. C., Transfection of aqueous CdS quantum dots using polyethylenimine. *Nanotechnology* **2008**, *19* (47), 475101.
70. Li, H.; Shih, W. Y.; Shih, W.-H., Synthesis and Characterization of Aqueous Carboxyl-Capped CdS Quantum Dots for Bioapplications. *Industrial & Engineering Chemistry Research* **2007**, *46* (7), 2013-2019.
71. Sadhu, S.; Patra, A., Lattice Strain Controls the Carrier Relaxation Dynamics in Cd<sub>x</sub>Zn<sub>1-x</sub>S Alloy Quantum Dots. *The Journal of Physical Chemistry C* **2012**, *116* (28), 15167-15173.
72. Sander F. Wuister; Meijerink, A., Synthesis and luminescence of CdS quantum dots capped with a silica precursor. *Journal of Luminescence* **2003**, *150* (1), 35-43.
73. Stroyuk, O.; Raevskaya, A.; Gaponik, N.; Selyshev, O.; Dzhegagan, V.; Schulze, S.; Zahn, D. R. T., Origin of the Broadband Photoluminescence of Pristine and Cu<sup>+</sup>/Ag<sup>+</sup>-Doped Ultrasmall CdS and CdSe/CdS Quantum Dots. *The Journal of Physical Chemistry C* **2018**, *122* (18), 10267-10277.



74. Marcu, L., Fluorescence Lifetime Techniques in Medical Applications. *Annals of Biomedical Engineering* **2012**, *40* (2), 304-331.
  75. Jackrel, M. E.; Cortajarena, A. L.; Liu, T. Y.; Regan, L., Screening Libraries To Identify Proteins with Desired Binding Activities Using a Split-GFP Reassembly Assay. *ACS Chemical Biology* **2010**, *5* (6), 553-562.
  76. Cortajarena, A. L.; Yi, F.; Regan, L., Designed TPR Modules as Novel Anticancer Agents. *ACS Chemical Biology* **2008**, *3* (3), 161-166.
  77. Grove, T.; Cortajarena, A.; Regan, L., Ligand binding by repeat proteins: natural and designed. *Current Opinion in Structural Biology* **2008**, *18* (4), 507-515.
  78. Bullen, C.; Mulvaney, P., The Effects of Chemisorption on the Luminescence of CdSe Quantum Dots. *Langmuir* **2006**, *22* (7), 3007-3013.
  79. Wei, H. H.-Y.; Evans, C. M.; Swartz, B. D.; Neukirch, A. J.; Young, J.; Prezhdo, O. V.; Krauss, T. D., Colloidal Semiconductor Quantum Dots with Tunable Surface Composition. *Nano Letters* **2012**, *12* (9), 4465-4471.
  80. Sowers, K. L.; Hou, Z.; Peterson, J. J.; Swartz, B.; Pal, S.; Prezhdo, O.; Krauss, T. D., Photophysical Properties of CdSe/CdS core/shell quantum dots with tunable surface composition. *Chemical Physics* **2016**, *471*, 24-31.
  81. Liu, W.; Greytak, A. B.; Lee, J.; Wong, C. R.; Park, J.; Marshall, L. F.; Jiang, W.; Curtin, P. N.; Ting, A. Y.; Nocera, D. G.; Fukumura, D.; Jain, R. K.; Bawendi, M. G., Compact Biocompatible Quantum Dots via RAFT-Mediated Synthesis of Imidazole-Based Random Copolymer Ligand. *Journal of the American Chemical Society* **2010**, *132* (2), 472-483.
  82. Wang, W.; Kapur, A.; Ji, X.; Safi, M.; Palui, G.; Palomo, V.; Dawson, P. E.; Mattoussi, H., Photoligation of an Amphiphilic Polymer with Mixed Coordination Provides Compact and Reactive Quantum Dots. *Journal of the American Chemical Society* **2015**, *137* (16), 5438-5451.
  83. Zhou, J.; Liu, Y.; Tang, J.; Tang, W., Surface ligands engineering of semiconductor quantum dots for chemosensory and biological applications. *Materials Today* **2017**, *20* (7), 360-376.
  84. Shen, L., Biocompatible Polymer/Quantum Dots Hybrid Materials: Current Status and Future Developments. *Journal of Functional Biomaterials* **2011**, *2* (4), 355-372.
  85. Wang, W.; Ji, X.; Kapur, A.; Zhang, C.; Mattoussi, H., A Multifunctional Polymer Combining the Imidazole and Zwitterion Motifs as a Biocompatible Compact Coating for Quantum Dots. *Journal of the American Chemical Society* **2015**, *137* (44), 14158-14172.
  86. Wuister, S. F.; de Mello Donegá, C.; Meijerink, A., Influence of Thiol Capping on the Exciton Luminescence and Decay Kinetics of CdTe and CdSe Quantum Dots. *The Journal of Physical Chemistry B* **2004**, *108* (45), 17393-17397.
  87. Liu, Y.; Kim, M.; Wang, Y.; Wang, Y. A.; Peng, X., Highly Luminescent, Stable, and Water-Soluble CdSe/CdS Core-Shell Dendron Nanocrystals with Carboxylate Anchoring Groups. *Langmuir* **2006**, *22* (14), 6341-6345.
  88. Fan, L.; Wang, P.; Guo, Q.; Lei, Y.; Li, M.; Han, H.; Zhao, H.; Yang, D.; Zheng, Z.; Yang, J., Improved stoichiometry and photoanode efficiency of thermally evaporated CdS film with quantum dots as precursor. *Nanotechnology* **2015**, *26* (33), 335606.
  89. Jiang, C.; Xu, S.; Yang, D.; Zhang, F.; Wang, W., Synthesis of glutathione-capped CdS quantum dots and preliminary studies on protein detection and cell fluorescence image. *Luminescence* **2007**, *22* (5), 430-437.
  90. Li, H.; Liu, J.; Yang, X., Facile Synthesis of Glutathione-capped CdS Quantum Dots as a Fluorescence Sensor for Rapid Detection and Quantification of Paraquat. *Analytical Sciences* **2015**, *31* (10), 1011-1017.
-

